



Particulate trace metal dynamics in response to increased CO₂ and iron availability in a coastal mesocosm experiment

M. Rosario Lorenzo¹, María Segovia¹, Jay T. Cullen², and María T. Maldonado³

¹Department of Ecology, Faculty of Sciences, University of Málaga, Bulevar Louis Pasteur, 29071 Málaga, Spain

²School of Earth and Ocean Sciences, University of Victoria, 3800 Finnerty Road, A405, Victoria BC V8P 5C2, Canada

³Department of Earth, Ocean and Atmospheric Sciences, University of British Columbia, 2207 Main Mall, Vancouver BC V6T 1Z4, Canada

Correspondence: María Segovia (segovia@uma.es) and María T. Maldonado (mmaldonado@eoas.ubc.ca)

Received: 14 October 2018 – Discussion started: 19 November 2018

Revised: 22 October 2019 – Accepted: 15 November 2019 – Published: 13 February 2020

Abstract. Rising concentrations of atmospheric carbon dioxide are causing ocean acidification and will influence marine processes and trace metal biogeochemistry. In June 2012, in the Raunefjord (Bergen, Norway), we performed a mesocosm experiment, comprised of a fully factorial design of ambient and elevated $p\text{CO}_2$ and/or an addition of the siderophore desferrioxamine B (DFB). In addition, the macronutrient concentrations were manipulated to enhance a bloom of the coccolithophore *Emiliania huxleyi*. We report the changes in particulate trace metal concentrations during this experiment. Our results show that particulate Ti and Fe were dominated by lithogenic material, while particulate Cu, Co, Mn, Zn, Mo and Cd had a strong biogenic component. Furthermore, significant correlations were found between particulate concentrations of Cu, Co, Zn, Cd, Mn, Mo and P in seawater and phytoplankton biomass ($\mu\text{gC L}^{-1}$), supporting a significant influence of the bloom in the distribution of these particulate elements. The concentrations of these biogenic metals in the *E. huxleyi* bloom were ranked as follows: $\text{Zn} < \text{Cu} \approx \text{Mn} < \text{Mo} < \text{Co} < \text{Cd}$. Changes in CO₂ affected total particulate concentrations and biogenic metal ratios (Me : P) for some metals, while the addition of DFB only significantly affected the concentrations of some particulate metals (mol L^{-1}). Variations in CO₂ had the most clear and significant effect on particulate Fe concentrations, decreasing its concentration under high CO₂. Indeed, high CO₂ and/or DFB promoted the dissolution of particulate Fe, and the presence of this siderophore helped in maintaining high dissolved Fe. This shift between particulate and dissolved Fe concentrations in the presence of DFB, promoted a massive

bloom of *E. huxleyi* in the treatments with ambient CO₂. Furthermore, high CO₂ decreased the Me : P ratios of Co, Zn and Mn while increasing the Cu : P ratios. These findings support theoretical predictions that the molar ratios of metal to phosphorous (Me : P ratios) of metals whose seawater dissolved speciation is dominated by free ions (e.g., Co, Zn and Mn) will likely decrease or stay constant under ocean acidification. In contrast, high CO₂ is predicted to shift the speciation of dissolved metals associated with carbonates such as Cu, increasing their bioavailability and resulting in higher Me : P ratios.

1 Introduction

Marine phytoplankton contribute half of the world's total primary productivity, sustaining marine food webs and driving the biogeochemical cycles of carbon and nutrients (Field et al., 1998). Annually, phytoplankton incorporate approximately 45 to 50 billion metric tons of inorganic carbon (Field et al., 1998), removing a quarter of the CO₂ emitted to the atmosphere by anthropogenic activities (Canadell et al., 2007). Yet, the atmospheric CO₂ concentration has increased by 40 % since pre-industrial times as a result of anthropogenic CO₂ emissions, producing rapid changes in the global climate system (Stocker et al., 2013). The dissolution of anthropogenic CO₂ in seawater causes shifts in the carbonate chemical speciation and leads to ocean acidification (OA) (Doney et al., 2009). Increased CO₂ in seawater may enhance or diminish phytoplankton productivity (Mackey et al., 2015), de-

crease the CaCO₃ production in most planktonic calcifiers (Riebesell and Tortell, 2011), and/or inhibit organic nitrogen and phosphorus acquisition (Hutchins et al., 2009). Thus, the biogeochemical cycling of nutrients is predicted to be highly affected by OA (Hutchins et al., 2009), as well as the distribution and speciation of trace metals in the ocean (Millero et al., 2009).

Trace metals, including Fe, Zn, Mn, Cu, Co and Mo, are essential for biological functions (e.g., photosynthesis, respiration and macronutrient assimilation), and Cd can supplement these functions. Trace metal availability can influence phytoplankton growth and community structure (Morel and Price, 2003). In turn, plankton control the distribution, chemical speciation and cycling of trace metals in the sea (Sunda, 2012), by, for example, releasing organic compounds that dominate the coordination chemistry of metals, internalizing trace elements into the cells and reducing and/or oxidizing metals at the cell surface. The chemistry of redox speciation of active trace metals is highly dependent on pH. Fe occurs in two main redox states in the environment, i.e., oxidized ferric Fe (Fe (III)), which is not very soluble at circumneutral pH, and reduced ferrous Fe (Fe (II)), which is more soluble in natural seawater but becomes rapidly oxidized (Millero et al., 1987). Fe speciation and bioavailability are dynamically controlled by the prevalent changing redox conditions. Also, as the ocean becomes more acidic, the ionic form of Cu (II) will be more easily reduced to Cu (I) (Millero et al., 2009). The effect of higher concentrations of Cu (I) in surface waters on biological systems is not well known. Therefore, while the effects of OA on inorganic metal speciation will be more pronounced for metals that form strong complexes with carbonates (e.g., copper) or hydroxides (e.g., Fe and aluminum), those that form stable complexes with chlorides (e.g., cadmium) will not be greatly affected. The pH mediated changes in concentrations and/or speciation could possibly enhance trace metal limitation and/or toxicity to marine plankton (Millero et al., 2009).

Fe is crucial for phytoplankton growth because it is involved in many essential physiological processes, such as photosynthesis, respiration and nitrate assimilation (Behrenfeld and Milligan, 2013). The decrease in seawater pH in response to OA may increase Fe solubility (Millero et al., 2009), but it may also result in unchanged or lower Fe bioavailability, depending on the nature of the strong organic Fe ligands (Shi et al., 2010). Consequently, changes in Fe bioavailability due to ocean acidification can positively or negatively affect ocean productivity and CO₂ drawdown. Copper is an essential micronutrient but may be toxic at high concentrations (Semeniuk et al., 2016). An increase in free cupric ion concentrations in coastal areas due to ocean acidification (Millero et al., 2009) could result in negative effects on phytoplankton. Given that trace metals are essential for phytoplankton productivity and that they are actively internalized during growth, it is important to study the impacts of

ocean acidification on the trace metal content of ecologically significant plankton species.

In a rapidly changing global environment, generated by anthropogenic CO₂ emissions, it is critical to gain adequate understanding about ecosystem responses. Due to the complex interactions in aquatic ecosystems, such predictions have so far not been possible based upon observational data and modeling alone. However, direct empirical studies of natural communities offer a robust tool to analyze interactive effects of multiple stressors. Specifically, mesocosm experiments allow perturbation studies with a high degree of realism compared to other experimental systems such as in the laboratory (highly controlled conditions, usually far from reality) or in situ in the ocean (where not all of the interactions are contemplated) (Riebesell et al., 2010; Stewart et al., 2013; Riebesell and Gattuso, 2015).

Emiliania huxleyi is the most cosmopolitan and abundant coccolithophore in the modern ocean (Paasche, 2002) and its growth and physiology has been studied under this experimental conditions (Segovia et al., 2017, 2018; Lorenzo et al., 2018). Furthermore, *E. huxleyi* has unique trace metal requirements relative to other abundant phytoplankton taxa (i.e., diatoms or dinoflagellates; Ho et al., 2003). Coccolithophores play a key role in the global carbon cycle because they produce photosynthetically organic carbon, as well as particulate inorganic carbon through calcification. These two processes foster the sinking of particulate organic carbon and trace metals and contribute to deep ocean carbon export (Hutchings, 2011) and ultimately to organic carbon burial in marine sediments (Archer, 1991; Archer and Maier-Reimer, 1994). However, ocean acidification will disproportionately affect the abundance of coccolithophores, as well as their rates of calcification and organic carbon fixation (Zondervan et al., 2007). In the present work, a bloom of the coccolithophorid *Emiliania huxleyi* was induced in a mesocosm experiment in a Norwegian fjord, where the speciation of particulate and dissolved trace metals is very dynamic (e.g., Fe; Öztürk et al., 2002). We aimed to examine and characterize the change of particle trace metals during an *E. huxleyi* bloom under the interactive effects of increased CO₂ and/or dissolved Fe.

2 Materials and methods

2.1 Experimental setup

The experimental work was carried out in June 2012 in the Raunefjord, off the coast of Bergen, Norway, as described in detail by Segovia et al. (2017). A total of 12 mesocosms (11 m³ each) were set up in a fully factorial design with all combinations of ambient and elevated CO₂ partial pressure (*p*CO₂) and dissolved iron (dFe) in three independent replicate mesocosms. The mesocosms were covered by lids (both transparent to PAR and UVR) and filled with fjord water

from 8 m depth. We achieved two CO₂ levels corresponding to present (390 ppm; low carbon, LC) and those predicted for 2100 (900 ppm; high carbon, HC) by adding different quantities of pure CO₂ gas (Schulz et al., 2009). The specific CO₂ concentration and the inlet flows in the mesocosms were measured by nondispersive infrared analysis by using a LI-COR (LI-820) CO₂ gas analyzer (LI-COR, Nebraska, USA). CO₂ concentrations in the mesocosms were calculated from pH and total alkalinity measurements using the CO₂sys software (Robbins et al. 2010). At the beginning of the experiment, nitrate (10 μM final concentration) and phosphate (0.3 μM final concentration) were added to induce a bloom of the coccolithophore *Emiliania huxleyi*, according to Egge and Heimdal (1994). Following recommendations by Marchetti and Maldonado (2016), to induce changes in Fe availability and analyze its effects on the plankton community, 70 nM (final concentration) of the siderophore desferrioxamine B (DFB) (+DFB and -DFB treatments) (Fig. S1b in the Supplement) was added to half of the mesocosms on day 7, when the community was already acclimated to high CO₂. The initial dFe concentration before DFB addition was about 4.5 nM (Fig. S3). Even though DFB is a strong Fe-binding organic ligand often used to induce Fe limitation in phytoplankton (Wells, 1999), DFB additions may also increase the dissolved Fe pool in environments with high concentrations of colloidal and/or particulate Fe, such as fjords (Kuma et al., 1996; Öztürk et al., 2002). By day 17, dissolved Fe concentrations were significantly higher (~ 3-fold) in the high CO₂ and DFB treatments than in the control (Fig S3b; Segovia et al., 2017). These results support an increase in the solubility of Fe in seawater by either lowering its pH (Millero et al., 2009) and/or the addition of DFB (Chen et al., 2004). The multifactorial experimental design consisted of triplicate mesocosms per treatment and the combinations of high and ambient pCO₂ and +DFB and -DFB, which resulted in a total of 12 mesocosms: LC-DFB (control), LC+DFB, HC+DFB and HC-DFB. Water samples from each mesocosm were taken from 2 m depth by gentle vacuum pumping of 25 L volume into acid-washed carboys by using vacuum pumps (PALL). Carboys were quickly transported to the on-shore laboratory. The biological and chemical variables analyzed were phytoplankton abundance and species composition, dissolved Fe and Cu concentrations (dFe, dCu), nutrient concentrations (nitrate, phosphate, silicic acid and ammonium) and particulate trace metal concentrations.

2.2 Dissolved copper (dCu)

Low-density polyethylene (LDPE) bottles were cleaned with 1 % alkaline soap solution for 1 week and then filled with 6 M trace metal grade HCl (Seastar, Fisher Chemicals) and submerged in a 2 M HCl bath for 1 month. For transport, they were filled with 1 M trace metal grade HCl for another month and kept double bagged. In between each acid treatment, the bottles were rinsed with Milli-Q water (Millipore; here-

after referred to as MQW). Before sampling, the bottles were rinsed three times with filtered seawater. Seawater was collected from each mesocosm, filtered through AcroPak[®] capsule filters with an 0.2 μm Supor[®] membrane into the trace-metal-clean LDPE bottles and acidified with ultra-clean trace metal grade HCl in a Class 100 laminar flow hood. Total dissolved Cu concentrations were measured following Zamzow et al. (1998) using a flow injection analysis chemiluminescence detection system (CL-FIA, Waterville Analytical). Total dissolved Fe concentrations were measured as described in Segovia et al. (2017) for this very experiment. The pH of the 0.2 μm filtered dFe samples was lowered to 1.7 by using Seastar HCl upon collection. Lowering the pH to 1.7 using HCl for more than 24 h ensures solubilization of all the Fe in the sample, as well as the release of all the Fe bound within strong organic complexes (such as Fe-DFB), thus making all dFe available for analysis (Johnson et al., 2007). During FIA-CL, the sample is only buffered to a higher pH immediately before entering the flow cell, right in front of the photomultiplier, thus Fe-DFB complexing kinetics are sufficiently slow to allow total dFe to be measured.

2.3 Particulate metals (pMe)

2.3.1 Sampling

All equipment and sampling material used during this study was rigorously acid-washed under trace-metal-clean conditions and protocols according to GEOTRACES. The material was cleaned with Milli-Q water (MQW) and 10 % Extran (Fisher Chemicals) at 60 °C for 6 h, followed by three thorough rinses with MQW at room temperature. The material was then cleaned with 10 % trace metal grade HCl (Sigma-Aldrich) at 60 °C for 12 h and then rinsed thoroughly five times with MQW at room temperature. The material was then covered by plastic and transported to the raft. Sampling in the raft was carried out under a mobile plastic cover hood. Filters were pre-cleaned with 10 % trace metal grade hydrochloric acid (Seastar, Fisher Chemicals) at 60 °C overnight and were rinsed with MQW. Seawater samples (1–3.5 L) were filtered gently onto 0.45 μm acid-washed Supor[®] –450 filters (within a trace-metal-clean Swinnex filter holder) on days 12, 17 and 21 of the experiment. Four technical replicates were taken from each mesocosm. Two filters were stored without an oxalate–ethylenediaminetetraacetic (EDTA) acid wash and the other two were individually washed with an oxalate-EDTA reagent to remove extracellular Fe, as well as other metals (Tang and Morel, 2006). Immediately following filtration, the treated filters were soaked with 20 mL of EDTA-oxalate solution and added to the headspace of the Swinnex holders with an acid-washed polypropylene syringe. After 10 min, a vacuum was applied to remove the oxalate solution and 10 mL of 0.2 μm filtered chelexed synthetic oceanic water (SOW) solution was passed through the filter to rinse off any remaining oxalate solution. Replicate filters

that were not treated with oxalate solution were transferred directly to 2 mL centrifuge polypropylene tubes for storage. The filters with particles were frozen in acid-washed 2 mL polypropylene tubes and then dried and stored until analysis.

2.3.2 Analytical methods

Filters were digested in 7 mL acid-washed Teflon (Teflon, Rochester, NY, USA) vials. Teflon vials were also precleaned using 10 % trace metal hydrochloric acid (Fisher, trace metal grade) over 2 d and then with nitric acid (Fisher, trace metal grade) at 70 °C over 3 d. In between each acid treatment, the bottles were rinsed with MQW. Samples were digested in 3 mL of HNO₃ and 0.5 mL of Hydrofluoric acid (HF; Fisher, trace metal grade) with lids on for 1 h on a hot plate at 200 °C. The lids were then removed to evaporate HF at 200 °C. After this, 1.5 mL of HNO₃ was added and the samples with lids on were heated overnight at 150 °C. Finally, 2.25 mL of HClO₄ (Fisher, Optima grade) was added and the samples were heated for 4 h at 200 °C. After complete digestion, the samples were dried on hot plates at 200 °C. The dried samples were dissolved in 1 % nitric acid with 1 ppb In internal standard. The analysis was performed using a high-resolution inductively coupled plasma mass spectrometer (ICP-MS, Element XR, Thermo Scientific) and the described instrumental settings (Table S1 in the Supplement). Filter blanks were collected and subjected to the same storage, digestion, dilution and analysis processes, and these blank values were subtracted from sample measurements. Particulate samples for ICP-MS analysis were processed in a trace-metal-free laboratory under a laminar flow fume hood.

2.3.3 The effect of oxalate-EDTA wash on particulate trace metal concentrations

To better estimate the biogenic fraction of the particulate metals, the filters were washed with an oxalate-EDTA solution, which removes extracellular metals and oxyhydroxides (Tovar-Sanchez et al., 2003; Tang and Morel, 2006).

In our study, the oxalate wash significantly decreased the concentration of all particulate metals, with the exception of Al and Ti (Tables S2 and S3), as observed by Rauschenberg and Twining (2015). The quantity of metal remaining after the oxalate wash (i.e., biogenic fraction) varied among elements (Tables S2 and S3). In general, the concentrations of Fe and Co in the particles were decreased the least by the oxalate wash (~ 25 %), while Mo and Pb concentrations were decreased the most (~ 70 %). The concentrations of particulate Cu, Zn, Cd and Mn were reduced by 50 % by the oxalate wash. As shown previously (Sanudo-Wilhelmy et al., 2004), the oxalate reagent also removed extracellular P (~ 20 %, Tables S2 and S3). Compared to Rauschenberg and Twining (2015), the estimates of the biogenic fraction, after the oxalate wash, were in agreement for Co, Cu and P and lower for Fe, Mn, Zn and Cd concentrations.

However, the efficacy of the oxalate wash to dissolve Fe and other metals from lithogenic particles is not well constrained (Frew et al., 2006; Rauschenberg and Twining, 2015; King et al., 2012). Therefore, the results obtained after the oxalate-EDTA wash should be interpreted with caution because we do not know whether the removed metal fraction is (a) only lithogenic or (b) mainly lithogenic but some biogenic fraction is also removed or (c) metals adsorbed onto particles are equally labile to the wash on biogenic and lithogenic particles. Given that many of the trends we observed were identical for the oxalate-EDTA washed and non-washed particles i.e., higher Me concentrations in the LC+DFB treatments (Tables S2 and S3) and positive correlations between phytoplankton biomass and Me concentrations (Lorenzo-Garrido, 2016), below we present and discuss only the non-oxalate wash results.

2.4 Statistical analyses

Data were checked for normality (by the Shapiro–Wilk test), homoscedasticity (by Levene’s test) and sphericity (by Mauchly’s test). All data met the requirements to perform parametric tests. Statistical significance of treatment effects was carried out using a split-plot ANOVA, followed by post hoc Sidak and Bonferroni tests (considering $P < 0.05$ as significant). All analyses were performed using the General Linear Model (GLM) procedure. The correlation between variables was analyzed by Pearson’s product moment multiple comparisons (considering $P < 0.05$ as significant). Statistical analyses were carried out using SPSS v22 (IBM statistics) and Sigmaplot 12 (Systat Software, Chicago, USA).

3 Results

3.1 Biological and chemical characteristics during the bloom

Plankton community dynamics and their response to the applied treatments in the mesocosms are described in detail by Segovia et al. (2017). Briefly, at the beginning of the experiment (days 1–10), a bloom of large chain-forming diatoms was observed, which declined by day 7 (Fig. S1g). This diatom bloom decline was associated with a sharp decrease in nitrate and silicic acid concentrations (Fig. S2; see Segovia et al., 2017 for further details). Picoeukaryotes dominated the phytoplankton community on day 8 (Fig. S1d). During the first 10 d of the experiment, there were no significant differences in the chemical variables measured between the treatments (Figs. S3 and S2). On day 7, half of the mesocosms were amended with DFB (+DFB treatments). Between days 7 and 17, an increase in dFe was observed in all treatments, except in the control (Fig. S3). This increase in dFe was sustained for the entire experiment in the DFB treatments (Fig. S3). Dissolved Cu concentrations were not affected by the different treatments (Fig. S3). After day 10, a

massive bloom of the coccolithophore *E. huxleyi* developed under LC+DFB condition (Fig. S1b), outcompeting the rest of the plankton groups (Fig. S1). This bloom was observed neither in the control treatment (LC-DFB) nor in the HC treatments, although *E. huxleyi* was still the most abundant species in all treatments, with the exception of the HC-DFB treatment (Fig. S1b).

3.2 Particulate metal concentrations during the mesocosm experiment

The pMe concentrations (nM, mean of all treatments and dates) during the experiment were highest for Al, Fe and Zn and lowest for Cd, following the trend of $Al \approx Fe \approx Zn < Ti < Cu \approx Mn < Mo \approx Pb < Co < Cd$ (Fig. 1, Table S2). Significant changes over time were observed for all particulate trace metal concentrations (Fe, Cu, Co, Zn, Cd, Mn, Mo and Pb) except Ti and Al (Fig. 1, Table 1). The only metal that showed a significant time-dependent decrease in its particulate concentration was Fe (Fig. 1, Table 1). In general, the treatments with the highest particulate metal concentrations also exhibited the highest particulate P, except for Al, Ti, Fe and Pb (Fig. 1, Table S2). On days 12 and 17, the highest particulate metal concentrations were observed in the LC+DFB treatment, while on day 21 they were observed in both LC treatments (Fig. 1, Table S2).

3.3 The effects of increased CO₂ and the DFB addition on particulate metal concentrations

Increased CO₂ and the DFB addition did not significantly affect the concentrations of particulate Al, Ti, Cu and Pb (Tables 1 and S2). Similarly, the addition of DFB did not directly influence particulate concentrations of Fe, but high CO₂ had a significant negative impact on particulate Fe (Tables 1 and S2, Fig. 1). Particulate Cd concentrations were also inversely affected by CO₂ but only in the presence of DFB (CO₂ and CO₂ × DFB effect: Tables 1 and S2, Fig. 1). All other elements (P, Co, Zn, Mn and Mo) exhibited significant effects due to CO₂ and DFB, but there was also a significant interaction between these two factors (Table 1, S2). This indicates that, for example, particulate Mn, Zn, Mo, Co and P concentrations were significantly decreased by high CO₂ but only in the +DFB treatments (Fig. 1, Tables 1, S2). Similarly, the addition of DFB significantly increased pZn and pMn but only at ambient CO₂ levels (Fig. 1, Tables 1, S2).

3.4 Phosphorous-normalized metal ratios in particles collected from the mesocosms and the effects of increased CO₂ and the DFB addition on these ratios

The P-normalized metal ratios (Fig. 2 and means in Table 2) were highest for Al and Fe (means of 70 ± 38 mmol Al : mol P and 39 ± 34 mmol Fe : mol P, respectively) and lowest for Cd

and Co (means of 0.02 ± 0.01 mmol Cd : mol P and 0.07 ± 0.02 mmol Co : mol P, respectively). Fe : P and Ti : P were not significantly affected by increased CO₂ and/or the DFB addition but showed a significant decrease over time (Table 3). The P-normalized Cu, Co and Zn ratios changed significantly over time (Table 3). Increased CO₂ significantly decreased Co, Zn and Mn : P ratios, while it increased Cu : P ratios (Fig. 2, Table 3). DFB did not affect the Me : P ratios of any of these bioactive elements (Table 3).

4 Discussion

4.1 The effects of CO₂ and dFe on the plankton community

In this experiment we investigated changes in particulate trace metal concentrations in response to increased CO₂ and/or an addition of the siderophore DFB in a coastal mesocosm experiment. For a better understanding of the processes affecting these stressors, we briefly summarize the mesocosm experiment results originating from Segovia et al. (2017). High CO₂, as well as the DFB addition, elevated the dFe concentration (Fig. S3c, increasing Fe availability (see Segovia et al., 2017 for further details). The higher dFe concentrations were sustained in the DFB treatments, suggesting that DFB significantly increased the solubility of Fe, as previously shown (Chen et al., 2004). A bloom of the coccolithophore *Emiliana huxleyi* was observed in the ambient CO₂ treatments and was especially massive in the presence of DFB (LC+DFB). Our results suggest that *E. huxleyi* is able to utilize DFB-bound Fe (Fe-DFB). Indeed, *E. huxleyi* has been shown to produce a wide range of organic compounds with high affinity for Fe (Boye and van den Berg, 2000). Furthermore, *E. huxleyi* is able to acquire Fe from organic Fe complexes (Hartnett et al., 2012), including Fe-DFB (Shaked and Lis, 2012; Lis et al., 2015). Indeed, the biomass of *E. huxleyi* was negatively affected by increased CO₂. However, increased dFe partially mitigated the negative effect of elevated CO₂, indicating that the coccolithophore was able to acclimate better to ocean acidification when Fe availability was high. High dFe also had a positive effect on the cyanobacterium *Synechococcus* sp., while the rest of the plankton food web did not respond to the treatments (Segovia et al., 2017).

4.2 Particulate Fe and Ti are associated with lithogenic sources, while particulate Co, Cu, Zn, Cd, Mo and Mn are associated with biogenic sources

The particulate trace metal concentrations (nM, mean of all treatments and dates) during the experiment were highest for Al, Fe and Zn and lowest for Co and Cd, following the trend of $Al \approx Fe \approx Zn < Ti < Cu \approx Mn < Mo \approx Pb < Co < Cd$ (Fig. 1). Lithogenic particles are enriched in Al and low in P (average crustal Al and P content is 2.9 mmol Al and

Table 1. Statistical analyses (split-plot ANOVA) of the effects of high CO₂, the addition of DFB and their interaction, as well as the effect of time, on the concentrations of particulate metals (nmol L⁻¹; see data in Table S2 and Fig. 1) in particles collected from the different mesocosm treatments. We used all of the days for the analyses because the split-plot ANOVA integrates fixed factors (CO₂ and DFB) and a repeated measures factor (time) by using the post hoc Bonferroni test, thus time was fully considered during the whole experimental period.

Factor	Al	Ti	P	Fe	Cu	Co	Zn	Cd	Mn	Mo	Pb
CO ₂	ns	ns	**	*	ns	**	***	***	**	***	ns
DFB	ns	ns	*	ns	ns	*	**	ns	*	*	ns
CO ₂ × DFB	ns	*	**	ns	ns	*	**	*	**	**	ns
Time	ns	ns	ns	***	*	***	***	***	***	***	**

ns: not significant. * $p < 0.05$. ** $p < 0.01$. *** $p < 0$.

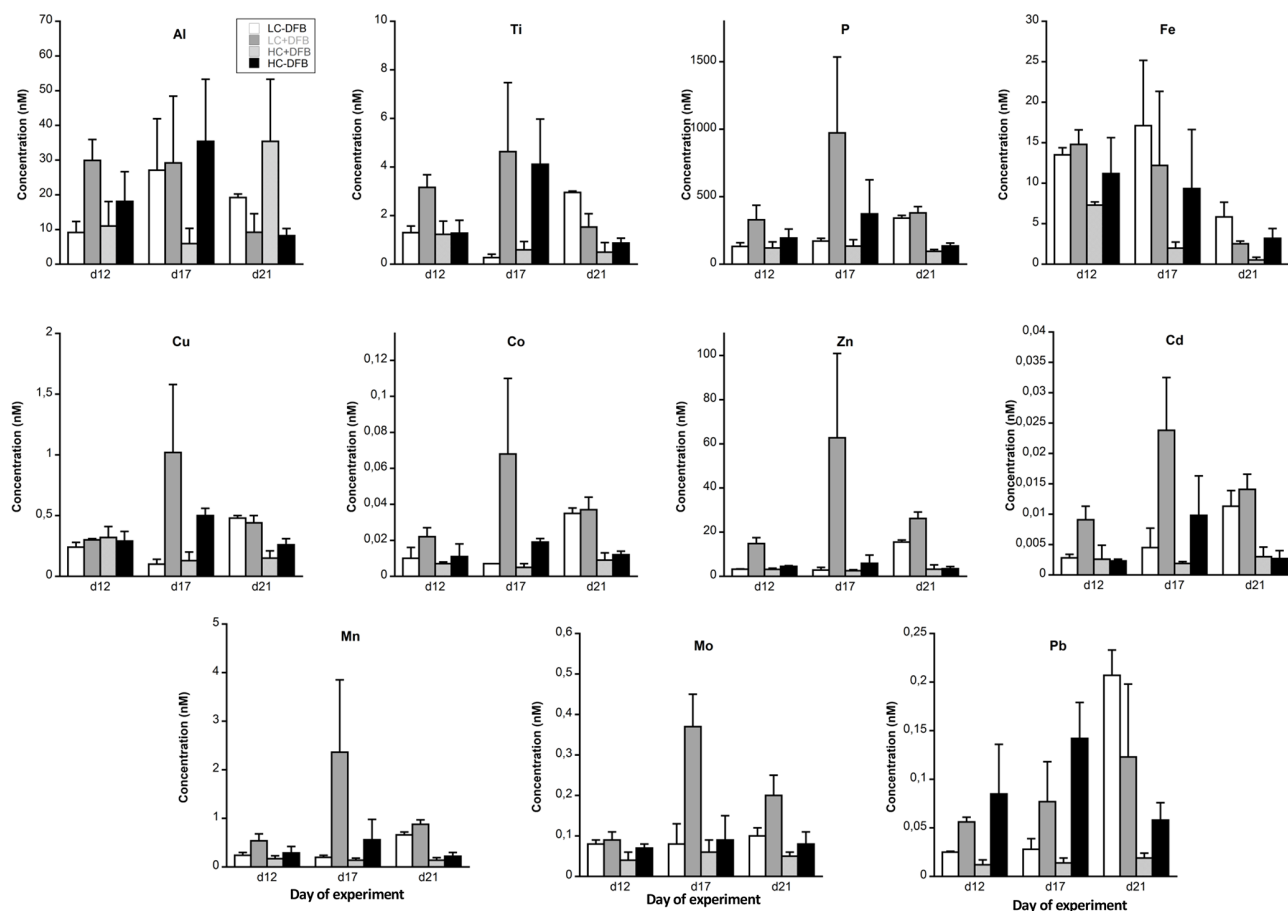


Figure 1. The concentration of particulate metals in seawater (nM) in the different treatments. LC: ambient CO₂ (390 μ atm); HC: increased CO₂ (900 μ atm). -DFB and +DFB are the ambient dFe and increased dFe, respectively, during the development of a bloom of *Emiliania huxleyi*. Bars are means of measurements in three independent mesocosms ($n = 3$) except for LC-DFB where $n = 2$. Error bars indicate SD.

0.034 mmol P g⁻¹ dry weight, Taylor, 1964), while biogenic particles are enriched in P and low in Al (average plankton Al and P content is 0.001 mmol Al and 0.26 mmol P g⁻¹ dry weight, Bruland et al., 1991). Therefore, the distinct high abundance of Al and P in lithogenic and biogenic particles, respectively, can be used to evaluate the relative contribution of lithogenic and biogenic material in our particulate samples. In order to do this, first it is important to establish that

the vast majority of the measured particulate P is associated with the biogenic fraction. In this study, the abiotic P was estimated using the particulate Al concentrations (nM) and the P:Al ratio in crustal material and was calculated to be negligible (< 1% of the total measured particulate P). In addition, a significant correlation ($p < 0.003$) was found between particulate phosphate concentrations and phytoplankton biomass (Table 4). Therefore, we assume

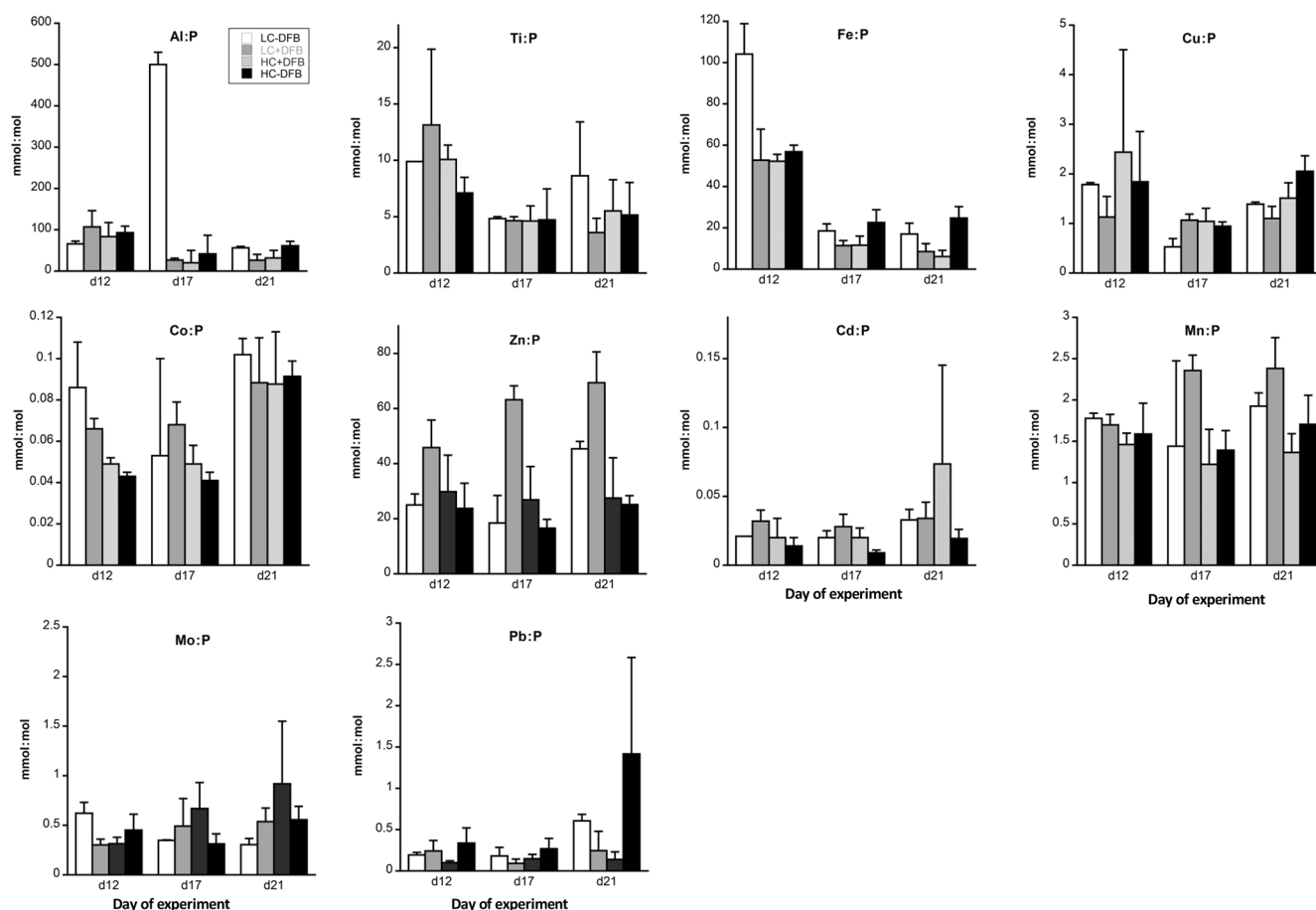


Figure 2. P-normalized metal quotas (mmol : mol P) of particles from different treatments. LC: ambient CO₂ (390 μatm); HC: increased CO₂ (900 μatm). -DFB and +DFB are the ambient dFe and increased dFe during the development of a bloom of *Emiliania huxleyi*, respectively. Bars are means of measurements in three independent mesocosms ($n = 3$) except for LC-DFB where $n = 2$. Error bars indicate SD.

Table 2. The average metal ratios in the particles collected in this study (without oxalate wash) using the data reported in Table S2. The P-normalized ratios (mmol : mol P, Fig. 2) are compared to previous estimates in marine plankton samples and phytoplankton cultures (a). The Al-normalized ratios (mmol : mol Al) are compared to crustal ratios (b).

(a)									
(mmol : mol P)	Mn : P	Fe : P	Co : P	Cu : P	Zn : P	Cd : P	Mo : P	Al : P	Reference
Phytoplankton _{Lab}	3.8	7.5	0.19	0.38	0.8	0.21	0.03		Ho et al. (2003)
Marine Plankton _{Field}	0.68 ± 0.54	5.1 ± 1.6	0.15 ± 0.06	0.41 ± 0.16	2.1 ± 0.88				Ho (2006)
<i>E. huxleyi</i> _{Lab}	7.1 ± 0.36	3.5 ± 0.07	0.29 ± 0.02	0.07 ± 0.013	0.38 ± 0.002	0.36 ± 0.01	0.022 ± 0.0003		Ho et al. (2003)
This study	1.65 ± 0.41	39.2 ± 34.3	0.07 ± 0.02	1.41 ± 0.55	34.02 ± 18.05	0.02 ± 0.01	0.42 ± 0.12	70 ± 38	
Crust ratio	510	29 738	13	25	32	0.05	0.46	89 972	Taylor (1964)
(b)									
(mmol : mol Al)	Mn : Al	Fe : Al	Co : Al	Cu : Al	Zn : Al	Cd : Al	Mo : Al	Pb : Al	Ti : Al
Crustal ratio	5.7	331	0.14	0.27	0.35	0.001	0.005	0.02	Taylor (1964)
This study	35 ± 28	506 ± 342	1.5 ± 1.2	26.5 ± 15	795 ± 865	0.5 ± 0.4	8.6 ± 6.5	4.9 ± 3.9	119 ± 47.6

Table 3. Statistical analyses (split-plot ANOVA) of the effects of CO₂, DFB and their interaction, as well as the effect of time, on the P-normalized metal quotas (mmol : mol P; see data in Fig. 2 and Table S2) in particles collected from the different mesocosm treatments.

Factor	Fe : P	Cu : P	Co : P	Zn : P	Cd : P	Mn : P	Mo : P	Pb : P	Ti : P
CO ₂	ns	*	***	**	ns	*	ns	ns	ns
DFB	ns	ns	ns	ns	ns	ns	ns	ns	ns
CO ₂ × DFB	ns	ns	ns	ns	ns	ns	ns	ns	ns
Time	***	***	***	***	ns	ns	ns	ns	***

ns: not significant. * $p < 0.05$. ** $p < 0.01$. *** $p < 0.001$.

a constant trace metal composition in biogenic particles (assuming they are rich in phytoplankton) and lithogenic particles (assuming they are rich in crustal material). We then calculated the expected metal concentrations in the particulate samples, assuming that all the P measured in the particles is associated with a biogenic fraction and that all Al in the particles is associated with the lithogenic fraction. Thus, for a given trace metal, its expected particulate trace metal concentration in seawater (mol L⁻¹) can be calculated as the sum of the contribution from biogenic and lithogenic particles, so that

$$[\text{Me}] = a [\text{P}] + b [\text{Al}],$$

where [Me] is the total concentration of the metal (mol L⁻¹) expected in the particulate sample, [P] is the P concentration measured in the particles (mol L⁻¹), [Al] is the Al concentration measured in the particles (mol L⁻¹), a is the average, well-known metal content in biogenic particles, normalized to P (i.e., mol Me : mol P in marine plankton, Ho, 2006) and b is the average, well-known metal content in lithogenic particles, normalized to Al (mol Me : mol Al in the Earth's crust; Taylor, 1964). For example, on day 21 in the HC-DFB treatment, the concentrations of particulate Al and P were 8.22 and 134.8 nM, respectively (Table S2). Assuming a constant 0.0051 mol Fe : mol P in biogenic particles (Ho, 2006) and 0.331 mol Fe : mol Al in lithogenic particles (Taylor, 1964; Table 2), we calculated an expected particulate Fe concentration of 3.41 nM, where 80 % was associated with lithogenic material and 20 % with biogenic material. Similar calculations were made for the bioactive metals Mn, Co, Cu, Zn, Cd and Mo (Table S4). Our calculations indicate that, on average, particulate Fe was dominated by the lithogenic component (accounting for an average of 78 % of the total expected particulate Fe), while for particulate Co, Cu, Zn, Cd and Mo the biogenic fraction dominated (accounting for 94, 95, 99, 94 and 98 %, respectively, of the total expected concentration; Table S4). Particulate concentrations of Mn were also dominated by the biogenic fraction (65 % of the total), but the lithogenic fraction was also significant (35 %). Moreover, the expected particulate Mn and Fe concentrations closely matched the particulate Mn and Fe concentration we measured (accounting for an average of ~ 71 % of the measured Mn and 115 % of the measured Fe). For other metals

(i.e., Cu, Mo and Zn), the expected particulate concentrations (nM) were lower than measured (23 % of the measured pCu and 8 % of measured pZn; Table S4). This suggests that the particles were enriched in Cu, Mo and Zn relative to what is expected based on natural marine plankton metal quotas (Bruland et al., 1991) and crustal ratios (Taylor, 1964).

To further establish the lithogenic or biogenic source of the pMe in the particles, the particulate metal concentrations were normalized to the concentrations of particulate P and Al (Fig. 2, Table 2). These ratios were then compared with well-known molar ratios of metal to Al in the crust (Taylor, 1964) and of metal to P ratios in marine plankton samples (Ho, 2006) and cultures (Ho et al., 2003) (Table 2). The average Fe : Al (506 mmol Fe : mol Al) and Ti : Al ratios (119 mmol Ti : mol Al; Table 2) were relatively similar to crustal molar ratios (331 mmol Fe : mol Al and 39 mmol Ti : mol Al; Taylor, 1964). Additional evidence for the significant lithogenic component in particulate Ti and Fe was gathered from Fig. 3, where we plotted the molar ratios of the metals relative to P in the collected particles against the Al : P ratios measured in those same particles. The slope of these data ((Me : P)/(Al : P) = mol Me : mol Al) is the ratio of Me : Al in the particles and can be compared to well-known Me : Al crustal ratio. Visually, if the data nicely fit the Me : Al line for crustal material, these metals are mainly associated with the lithogenic component, as evident for Fe and Ti (Fig. 3). These combined results suggest that, in our experiment, particulate Fe and Ti concentrations were enriched by lithogenic material. In support of this finding, we also found no significant correlation between particulate Fe and Ti concentrations (nM) and either the total plankton (phytoplankton and microzooplankton) or *E. huxleyi* biomass (µg CL⁻¹; Table 4).

In contrast, when the P-normalized metal ratios in the particles collected from the mesocosms were plotted against the Al : P ratios in these particles, there were no correlations for the following metals: Co, Cu, Zn, Cd, Mn and Mo (Fig. 3). This indicates that these particulate metals were not enriched in lithogenic material. Our measured metal : P ratios were comparable to plankton ratios in natural samples and in cultures (Table 2). The concentrations (mol L⁻¹) of these metals (i.e., Cu, Co, Zn, Cd, Mn and Mo), as well as P, also showed significant correlations with the biomass (µg CL⁻¹)

Table 4. The relationship (Pearson correlations, $p < 0.05$) between particulate metal concentrations (nmol L^{-1} , no oxalate wash, reported in Table S2) and the biomass (μgCL^{-1}) of *Emiliana huxleyi* and total cells (phytoplankton and microzooplankton) collected from the different mesocosm treatments.

		P	Fe	Cu	Co	Zn	Cd	Mn	Mo	Pb	Ti
<i>E. huxleyi</i>	Correlation coefficient	0.622		0.614	0.756	0.747	0.818	0.686	0.825		
	p value	0.003	ns	0.003	7.35×10^{-5}	1.01×10^{-4}	6.02×10^{-6}	5.93×10^{-4}	4.20×10^{-6}	ns	ns
Total cells	Correlation coefficient	0.641		0.51	0.644	0.889	0.802	0.598	0.53		
	p value	0.002	ns	0.02	1.62×10^{-3}	7.03×10^{-8}	1.23×10^{-5}	4.18×10^{-3}	1.35×10^{-2}	ns	ns

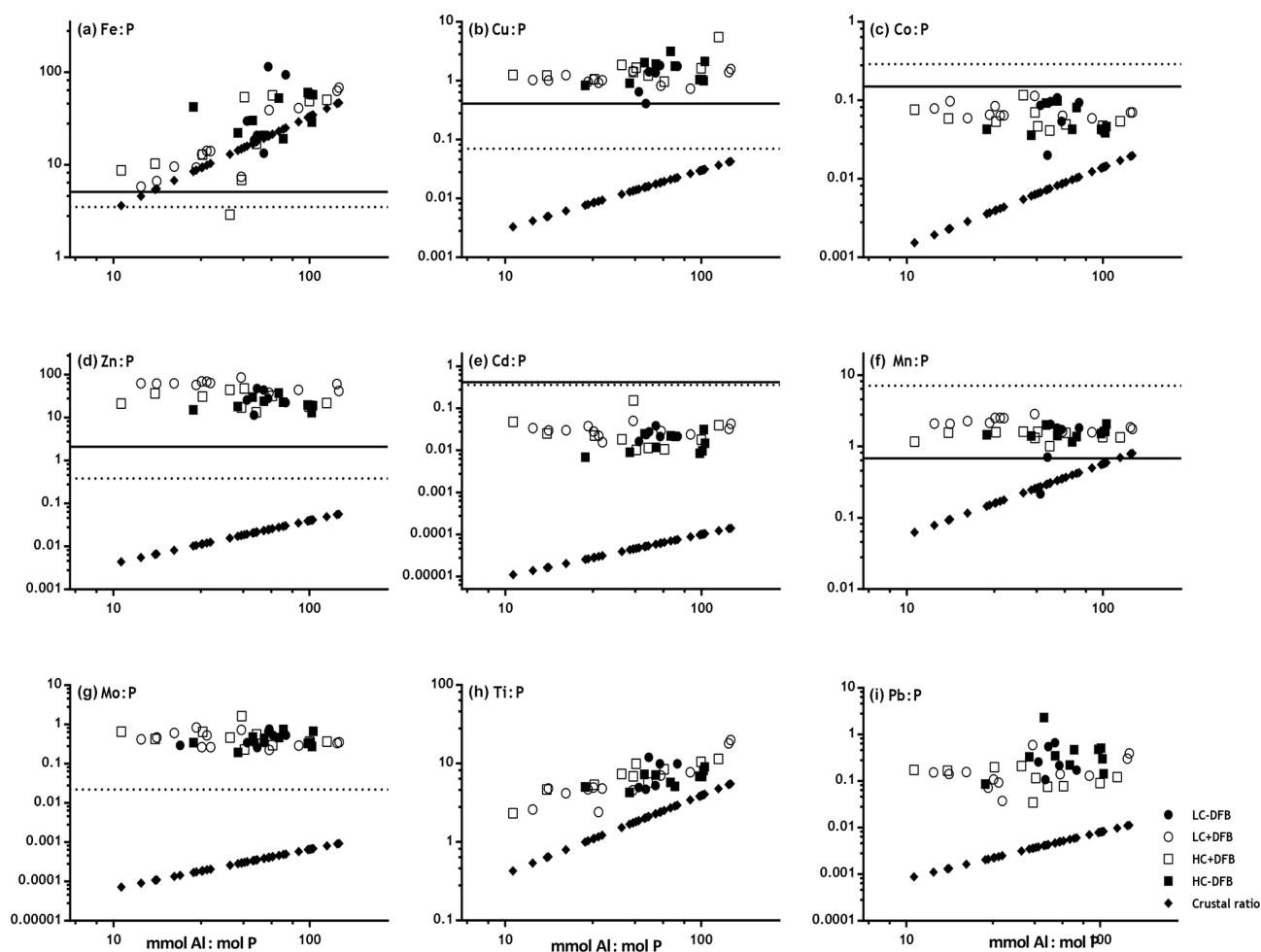


Figure 3. Comparison of P-normalized metal ratios in particles ($\text{mmol} : \text{mol P}$) against $\text{mmol Al} : \text{mol P}$ ratios in the same particles (without oxalate wash) collected from the different mesocosm treatments (LC: ambient CO_2 ; HC: increased CO_2 ($900 \mu\text{atm}$); -DFB: no DFB addition; +DFB: with a 70 nM DFB addition) during the development of a bloom on days 12, 17 and 21 (original data reported in Table S2). The parallel solid and dotted lines on the x axis represent the average metal quotas obtained from marine plankton assemblages (Ho, 2006) and from cultures of *Emiliana huxleyi* (Ho et al., 2003). The slope of the line with the \blacklozenge symbols indicates the average metal : Al ($\text{mol} : \text{mol}$) in crustal material (Taylor, 1964). (a) Fe : P, (b) Cu : P, (c) Co : P, (d) Zn : P, (e) Cd : P, (f) Mn : P, (g) Mo : P, (h) Ti : P, (i) Pb : P.

of *E. huxleyi* and that of total plankton cells ($p < 0.05$, Table 4), supporting a significant influence of the phytoplankton in the distribution of these particulate elements.

4.3 Particulate metals with a strong biogenic component: their P-normalized ratios

The concentrations of particulate bioactive metals (mol L^{-1}) with a significant biogenic component (i.e., excluding Fe) in the studied *E. huxleyi* bloom were ranked as follows: $\text{Zn} < \text{Cu} \approx \text{Mn} < \text{Mo} < \text{Co} < \text{Cd}$ (Fig. 1, Table S2). This is similar to those reported in indigenous phytoplankton populations, i.e., $\text{Fe} \approx \text{Zn} < \text{Cu} \approx \text{Mn} \gg \text{Co} \approx \text{Cd}$ (Twining and Baines, 2013). The only treatment where *E. huxleyi* did not dominate the community was the HC-DFB; in this treatment the ranking of these biogenic particulate trace metals was the same as that of LC+DFB (with the massive *E. huxleyi* bloom), but their concentrations were lower than those in LC+DFB. At the end of the experiment, the concentrations of these biogenic metals were, in general, comparable in both HC treatments and lower than those in the LC treatments (Fig. 1, Table S2). Therefore, high CO_2 had a tendency to decrease particulate metal concentrations, especially on day 21. Given the strong correlation between concentrations of these particulate bioactive metals and phytoplankton biomass, the lower particulate concentrations in high CO_2 were mainly due to low phytoplankton biomass.

Particulate Zn concentrations were especially high in the LC+DFB treatment (Fig. 1), where the highest *E. huxleyi* biomass was observed. *Emiliania huxleyi* is well known for its high Zn cellular requirements ($\sim 1\text{--}10$ for *E. huxleyi* vs. $1\text{--}4$ $\text{mmol Zn} : \text{mol P}$ for other phytoplankton; Sunda and Huntsman, 1995b; Sunda, 2012), but the Zn:P ratios in the LC+DFB treatment (range of $45\text{--}69$ $\text{mmol Zn} : \text{mol P}$; Fig. 2, Table S2), as well as in all the other treatment (range of $16\text{--}34$ $\text{mmol Zn} : \text{mol P}$; Fig. 2, Table S2), were significantly higher than these published ratios. This could be explained by the adsorption of these metals to the outside of the cells and/or anthropogenic inputs of Zn into the fjord. The Zn:P ratios in the samples washed with the oxalate-EDTA were still high (range of $28\text{--}57$ for LC+DFB and $16\text{--}33$ $\text{mmol Zn} : \text{mol P}$ in all other treatments, Table S3), thus adsorption might have not been significant. We hypothesize that anthropogenic aerosols that are rich in anthropogenic particulate metals, such as Zn and Cu (Perry et al., 1999; Narita et al., 1999), and have high percentage of Zn and Cu dissolution might be the source of these high Zn concentrations and ratios in the particles.

Similarly, the Cu:P ratios in the collected particles were relatively elevated (1.4 ± 0.8 $\text{mmol Cu} : \text{mol P}$) compared to those of other phytoplankton, including *E. huxleyi* (Table 2). The dissolved (7.7 ± 0.41 nM Cu, Fig. S3) and particulate Cu concentrations (0.35 ± 0.25 nM, Table S2) in our experiment were high and similar to those previously measured in this fjord (Muller et al., 2005). Rain events (or wet deposition of

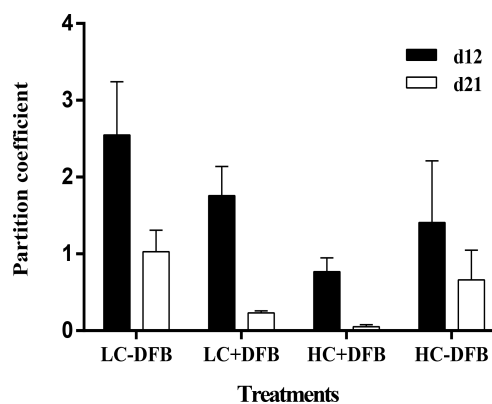


Figure 4. The Fe partition coefficients (the molar ratio between particulate and dissolved concentrations) in the different mesocosm treatments. LC: ambient CO_2 ($390 \mu\text{atm}$); HC: increased CO_2 ($900 \mu\text{atm}$). -DFB and +DFB are with no DFB addition and with a 70 nM DFB addition, respectively, on day 12 and day 21. Bars are means of measurements in three independent mesocosms ($n = 3$), except for LC-DFB, where $n = 2$. Error bars indicate SD.

anthropogenic aerosols) in this fjord result in high dissolved Cu and the active production of strong organic ligands by *Synechococcus* to lower the free Cu concentrations (Muller et al., 2005). Therefore, high Cu might be a general condition in this fjord due to the rainy nature of the geographical location, and indigenous plankton might have developed physiological mechanisms to deal with high Cu, such as the production of organic ligands to prevent uptake (Vraspir and Butler, 2009), or of heavy-metal-binding peptides (phytochelatins) to lower Cu toxicity inside the cell (Ahner and Morel, 1995; Ahner et al., 1995; Knauer et al., 1998). Since we measured high particulate Cu and Cu:P in our experiment, *E. huxleyi* might have been relying mainly on phytochelatins to buffer high intracellular Cu (Ahner et al., 2002).

The Cd:P ratios (average 0.024 ± 0.01 $\text{mmol Cd} : \text{mol P}$, Fig. 2) were significantly lower than those in phytoplankton and *E. huxleyi* (0.36 $\text{mmol Cd} : \text{mol P}$, Fig. 2). This was surprising because Cd quotas are normally higher in coccolithophores than in diatoms and chlorophytes (Sunda and Huntsman, 2000; Ho et al., 2003). High Cd quotas in coccolithophores have been suggested to result from accidental uptake through Ca transporters and channels (Ho et al., 2009). The low Cd quotas here may be explained by the antagonistic interaction between Mn and Cd or Zn and Cd under high Mn and Zn, respectively (Sunda and Huntsman, 1998, 2000; Cullen and Sherrell, 2005).

Since high Zn:P ratios were common in this study (34.02 ± 18.05 $\text{mmol Zn} : \text{mol P}$, Fig. 2), we hypothesize that high Zn levels antagonistically interacted with Cd, resulting in low Cd:P ratios in the particles.

4.4 The effects of increased CO₂ and the DFB addition on particulate metal concentrations and P-normalized ratios

Fe enrichment is common in coastal waters, due to sediment resuspension, river input, aeolian deposition, and mixing or upwelling of deep water. Indeed, Fe was the essential metal with the highest particulate concentrations in our study (Fig. 1, Table S2). Furthermore, in this study particulate Fe was characterized by a strong lithogenic component and was not correlated with phytoplankton biomass. Fe was also unique, in that it was the only trace element whose particulate concentration was significantly and exclusively affected by CO₂ (no interaction between CO₂ and DFB), regardless of the presence or absence of DFB (Table 1). Furthermore, particulate Fe concentrations (nM) decreased steadily between days 12 and 21, with the exception of the control treatment (LC-DFB; Fig. 1, Table S2). This suggests that the increase in CO₂ and/or the DFB addition reduce the concentration of pFe, despite the phytoplankton bloom. Such a decrease in pFe (ranging from 2.3-fold in LC-DFB to 13.7-fold in HC+DFB; Table S2) might be mediated by the dissolution of particulate Fe by low pH or by the presence of strong organic chelators (Segovia et al., 2017 and references therein), where dFe notably increased in treatments with high CO₂ and/or the addition of DFB (Fig. S3). Furthermore, the dissolution of particulate Fe in the treatments with high CO₂ and/or the addition of DFB was evident in the Fe partitioning coefficients of the molar ratio between particulate and dissolved concentrations (Fig. 4). On day 21, the Fe partitioning coefficients varied 22-fold between the highest for the control (LC-DFB: 1.039) and lowest for the HC+DFB treatments (HC+DFB: 0.047; Fig. 4). Thus, either the DFB addition or high CO₂ promoted the dissolution of pFe. However, at the end of the experiment, high dFe concentrations were only observed in the treatments with the DFB additions, suggesting that the presence of strong organic Fe chelators, such as DFB, mediated the maintenance of high dissolved Fe concentrations (Segovia et al., 2017). Thus, in our future oceans, high CO₂ (low pH) will increase dissolved Fe concentrations in regions rich in particulate Fe and strong organic Fe chelators. The deleterious effects of OA on the development of ecologically important species sensitive to increased CO₂, such as *E. Huxleyi*, will be less pronounced in high Fe environments than in Fe-limited environments.

In contrast to the findings for Fe, particulate Cu concentrations (a) were not affected by either high CO₂ or the DFB addition, (b) were dominated by a biogenic component, and (c) were significantly correlated with phytoplankton biomass (Table 4). Furthermore, unique to Cu was a significant increase in Cu:P ratios by day 21 in the high CO₂ treatments, especially when no DFB was added. Since the Cu partitioning coefficients only varied by 3.25 fold among treatments on day 21 (LC-DFB of 0.065 vs. HC+DFB of 0.047; data not shown), we hypothesize that high CO₂ did not affect the par-

tioning between particulate and dissolved Cu, but instead it affected the speciation of dissolved Cu, increasing free Cu (Cu²⁺) and thus its bioavailability. This resulted in the highest Cu:P ratios in the high CO₂ treatments, despite the low phytoplankton biomass. This increase in bioavailability under lower pH is typical of metals that form strong inorganic complexes with carbonates, such as Cu²⁺ (Millero et al., 2009). Thus, in our future oceans, high CO₂ (low pH) will shift the speciation of dissolved Cu towards higher abundance of free ionic species, increasing its bioavailability and likely its toxicity.

Similarly to Cu, particulate Co, Zn and Mn were correlated with biomass and were dominated by the biogenic component. But in contrast to Cu, these metal particulate concentrations were affected by increased CO₂ and/or the DFB addition. However, the effects of high CO₂ and/or DFB were very complex because significant interactions between these two factors were observed (Table 1); and further studies are required before we are able to discern and conclude a significant trend. Yet, the P-normalized ratios of Co, Zn and Mn were significantly affected by CO₂ (Table 3), exhibiting moderately lower ratios under high CO₂, when phytoplankton biomass was lowest. These results imply that the bioavailability of these metals was not enhanced under acidic conditions. This suggests that under high CO₂ (low pH) the free ionic species of these metals will not significantly increase in the future, as shown for metals that occur predominantly as free ionic species in seawater (Millero et al., 2009).

5 Concluding remarks

The results presented here show that, in the fjord where we carried out the present experiment, particulate Fe was dominated by lithogenic material and was significantly decreased in the treatments with high CO₂ concentrations and/or DFB addition. Indeed, high CO₂ and/or DFB promoted the dissolution of particulate Fe, and the presence of this strong organic complex helped in maintaining high dissolved Fe. This shift between particulate and dissolved Fe, in the presence of DFB, promoted a massive bloom of *E. huxleyi* in the treatments with ambient CO₂, due to increased dissolved Fe. During the bloom of *E. huxleyi*, the concentrations of particulate metals (mol L⁻¹) with a strong biogenic component (Cu, Co, Zn, Cd, Mn and Mo) were (a) highly dynamic, (b) positively correlated with plankton biomass and (c) influenced by growth requirements. Furthermore, high CO₂ decreased the Me:P ratios of Co, Zn and Mn, while increasing the Cu:P ratios. In contrast, DFB had no effects on these ratios. According to our results, high CO₂ may decrease particulate Fe and increase dissolved Fe, but high concentrations of dissolved Fe will only be maintained by the presence of strong organic ligands. Furthermore, ocean acidification will decrease *E. huxleyi* abundance and, as a result, the sinking of particulate metals enriched in *E. huxleyi*. Moreover, the

Me : P ratios of metals that are predominately present in an ionic free form in seawater (e.g., Co, Zn and Mn) will likely decrease or stay constant. In contrast, high CO₂ is predicted to shift the speciation of dissolved metals associated with carbonates, such as Cu, increasing their bioavailability and resulting in higher Me : P ratios. We suggest that high Cu might be a common condition in this fjord and that autochthonous plankton might be able to cope with high Cu levels by developing specific physiological mechanisms. Future high CO₂ levels are expected to change the relative concentrations of particulate and dissolved metals, due to the differential effects of high CO₂ on trace metal solubility, speciation, adsorption and toxicity, as well as on the growth of different phytoplankton taxa, and their elemental trace metal composition.

Data availability. Underlying research data can be accessed at: <https://doi.org/10.3354/meps12025> (Segovia et al., 2017).

Supplement. The supplement related to this article is available online at: <https://doi.org/10.5194/bg-17-757-2020-supplement>.

Author contributions. This research project was conceived by MS. MS designed the experiment with input from MM. JTC was instrumental in the analyses of the dissolved Fe and Cu samples. MRL and MM analyzed the samples, and MRL, MM, and MS processed the data. MS, MM, and MRL wrote the manuscript.

Competing interests. The authors declare that they have no conflict of interest.

Acknowledgements. We give special thanks to Francisco Jose Lazaro Osoro (Universidad de Zaragoza) for his help collecting the samples during the experiment. We thank the anonymous reviewers for their insightful comments and constructive criticism.

Financial support. This work was funded by CTM/MAR 2010-17216 (PHYTOSTRESS) research grant from the Spanish Ministry for Science and Innovation (Spain) to María Segovia and by NSERC grants (Canada) to María T. Maldonado and Jay T. Cullen. M. Rosario Lorenzo was funded by a FPU grant from the Ministry for Education (Spain) and by fellowships associated with the above-mentioned research grants to carry out a short stay at laboratories to analyze dissolved and particulate metals. We thank all the participants of the PHYTOSTRESS experiment for their collaboration and the MBS (Espérend, Norway) staff for logistical support during the experiment.

Review statement. This paper was edited by Koji Suzuki and reviewed by two anonymous referees.

References

- Ahner, B. A. and Morel, F. M. M.: Phytochelatin production in marine algae, 2. Induction by various metals, *Limnol. Oceanogr.*, 40, 658–665, <https://doi.org/10.4319/lo.1995.40.4.0658>, 1995.
- Ahner, B. A., Liping, W., Oleson, J. R., and Ogura, N.: Glutathione and other low molecular weight thiols in marine phytoplankton under metal stress, *Mar. Ecol. Prog. Ser.*, 232, 93–103, 2002.
- Archer, D.: Modeling the calcite lysocline, *J. Geophys. Res.*, 96, 17037–17050, 1991.
- Archer, D. and Maier-Reimer, E.: Effect of deepsea sedimentary calcite preservation on atmospheric CO₂ concentration, *Nature*, 367, 260–263, 1994.
- Behrenfeld, M. J. and Milligan, A. J.: Photophysiological expressions of iron stress in phytoplankton, *Ann. Rev. Mar. Sci.*, 5, 217–246, 2013.
- Boye, M. and van den Berg, C. M. G.: Iron availability and the release of iron-complexing ligands by *Emiliania huxleyi*, *Mar. Chem.*, 70, 277–287, 2000.
- Canadell, J. G., Quéré, C., Raupach, M. R., Field, C. B., Buitenhuis, E. T., Ciais, P., Conway, T. J., Gillet, N. P., Houghton, R. A., and Marland, G.: Contributions to accelerating atmospheric CO₂ growth from economic activity, carbon intensity, and efficiency of natural sinks, *P. Natl. Acad. Sci. USA*, 104, 18886–18870, 2007.
- Chen, M., Wang, W.-X., and Guo, L.: Phase partitioning and solubility of iron in natural seawater controlled by dissolved organic matter, *Global Biogeochem. Cy.*, 18, GB4013, <https://doi.org/10.1029/2003GB002160>, 2004.
- Cullen, J. T. and Sherrell, R. M.: Effects of dissolved carbon dioxide, zinc, and manganese on the cadmium to phosphorus ratio in natural phytoplankton assemblages, *Limnol. Oceanogr.*, 50, 1193–1204, 2005.
- Doney, S. C., Fabry, V. J., Feely, R. A., and Kleypas, J. A.: Ocean Acidification: The Other CO₂ Problem, *Annu. Rev. Mar. Sci.*, 1, 169–192, 2009.
- Edge, J. K. and Heimdahl, B. R.: Blooms of phytoplankton including *Emiliania huxleyi* (Haptophyta), Effect of nutrient supply in different N : P ratios, *Sarsia*, 79, 333–348, 1994.
- Field, C. B.: Primary production of the biosphere: Integrating terrestrial and oceanic components, *Science*, 281, 237–240, 1998.
- Frew, R. D., Hutchins, D. A., Nodder, S., Sanudo-Wilhelmy, S., Tovar-Sanchez, A., Leblanc, K., Hare, C. E., and Boyd, P. W.: Particulate iron dynamics during Fe Cycle in subantarctic waters southeast of New Zealand, *Global Biogeochem. Cy.*, 20, GB1S93, <https://doi.org/10.1029/2005GB002558>, 2006.
- Guo, J., Lapi, S., Ruth, T. J., and Maldonado, M. T.: The effects of iron and copper availability on the copper stoichiometry of marine phytoplankton, *J. Phycol.*, 48, 312–325, 2012.
- Hartnett, A., Böttger, L. H., Matzanke, B. F., and Carrano, C. J.: Iron transport and storage in the coccolithophore: *Emiliania huxleyi*, *Metallomics*, 4, 1127–1227, 2012.
- Ho, T.-Y.: The trace metal composition of marine microalgae in cultures and natural assemblages, in: *Algal cultures, analogues of blooms and applications*, edited by: Rao, S., Science Publishers, New Hampshire, 271–299, 2006.
- Ho, T.-Y., Quigg, A., Zoe, V., Milligan, A. J., Falkowski, P. G., and Morel, M. M.: The elemental composition of some marine phytoplankton, *J. Appl. Phycol.*, 159, 1145–1159, 2003.

- Ho, T.-Y., Wen, L.-S., You, C.-F., and Lee, D.-C.: The trace metal composition of size-fractionated plankton in the South China Sea: Biotic versus abiotic sources, *Limnol. Oceanogr.*, 52, 1776–1788, 2007.
- Ho, T.-Y., You, C. F., Chou, W.-C., Pai, S.-C., Wen, L.-S., and Sheu, D. D.: Cadmium and phosphorus cycling in the water column of the South China Sea: The roles of biotic and abiotic particles, *Mar. Chem.*, 115, 125–133, 2009.
- Hoffmann, L. J., Breitbarth, E., Boyd, P. W., and Hunter, K. A.: Influence of ocean warming and acidification on trace metal biogeochemistry, *Mar. Ecol. Prog. Ser.*, 470, 191–205, 2012.
- Hutchins, D., Mulholland, M., and Fu, F.: Nutrient cycles and marine microbes in a CO₂-enriched ocean, *Oceanography*, 22, 128–145, 2009.
- Hutchins, D. A.: Forecasting the rain ratio, *Nature*, 476, 41–42, 2011.
- Jakuba, R. W., Moffett, J. W., and Dyhrman, S. T.: Evidence for the linked biogeochemical cycling of zinc, cobalt, and phosphorus in the western North Atlantic Ocean, *Global Biogeochem. Cy.*, 22, GB4012, https://doi.org/10.1007/978-3-319-24945-2_8, 2008.
- Johnson, K. S., Boyle, E., Bruland, K., Coale, K., Measures, C., Moffet, J. et al.: Developing Standards for Dissolved Iron in Seawater, *EOS T. Am. Geophys. Un.*, 88, 131–132, 2007.
- King, A. L., Sañudo-Wilhelmy, S. A., Boyd, P. W., Twining, B. S., Wilhelm, S. W., Breene, C., Ellwood, M. J., and Hutchins, D. A.: A comparison of biogenic iron quotas during a diatom spring bloom using multiple approaches, *Biogeosciences*, 9, 667–687, <https://doi.org/10.5194/bg-9-667-2012>, 2012.
- Kuma, K., Nishioka, J., and Matsunaga, K.: Controls on iron(III) hydroxide solubility in seawater: the influence of pH and natural organic chelators, *Limnol. Oceanogr.*, 41, 396–407, 1996.
- Knauer, K., Ahner B., Han, B. X., and Sigg, L.: Environmental Toxicology and chemistry, Metal and phytochelatin content in phytoplankton from freshwater lakes with different metal concentrations, 17, 2444–2452, <https://doi.org/10.1002/etc.5620171210>, 1998.
- Lis, H., Shaked, Y., Kranzler, C., Keren, N., and Morel, F. M. M.: Iron bioavailability to phytoplankton: an empirical approach, *Isme J.*, 9, 1003–1013, 2015.
- Lorenzo, M. R. L., Iniguez, C., Egge, J., Larsen, A., Berger, S. A. B., Garcia-Gomez, C., and Segovia, M.: Increased CO₂ and iron availability effects on carbon assimilation and calcification on the formation of *Emiliania huxleyi* blooms in a coastal phytoplankton community, *Env. Exp. Bot.*, 148, 47–58, 2018.
- Lorenzo-Garrido, M. R.: Response of the coccolithophore *Emiliania huxleyi* to increased CO₂ and Fe availability within the plankton food web, PhD thesis, Universidad de Malaga (Spain), 2016.
- Mackey, K. R. M., Morris, J. J., and Morel, F. M. M.: Response of photosynthesis to ocean acidification, *Oceanography*, 28, 74–91, 2015.
- Marchetti, A. and Maldonado, M. T.: Iron, in: The physiology of microalgae, edited by: Borowitzka, M. A., Beardall, J., Raven, J. A., Springer International Publishing, 233–279, 2016.
- Millero, F. J., Sotolongo, S., and Izaguirre, M.: The oxidation kinetics of Fe(II) in seawater, *Geochim. Cosmochim. Ac.*, 51, 793–801, 1987.
- Millero, F. J., Woosley, R., Ditrolio, B., and Waters, J.: Effect of ocean acidification on the speciation of metals in seawater, *Oceanography*, 22, 72–85, 2009.
- Morel, F. M. and Price, N. M.: The biogeochemical cycles of trace metals in the oceans, *Science*, 300, 944–947, 2003.
- Muller, F. L., Larsen, A., Stedmon, C. A., and Søndergaard, M.: Interactions between algal – bacterial populations and trace metals in fjord surface waters during a nutrient-stimulated summer bloom, *Limnol. Oceanogr.*, 50, 1855–1871, 2005.
- Öztürk, M., Steinnes, E., and Sakshaug, E.: Iron speciation in the Trondheim Fjord from the perspective of iron limitation for phytoplankton, *Estuar. Coast. Shelf S.*, 55, 197–212, 2002.
- Paasche, E.: A review of the coccolithophorid *Emiliania huxleyi* (Pymnesiophyceae), with particular reference to growth, coccolith formation, and calcification-photosynthesis interactions, *Phycologia*, 40, 503–529, 2002.
- Rauschenberg, S. and Twining, B. S.: Evaluation of approaches to estimate biogenic particulate trace metals in the ocean, *Mar. Chem.*, 171, 67–77, 2015.
- Riebesell, U. and Tortell, P. D.: Effects of ocean acidification on pelagic organisms and ecosystems, edited by: Gattuso, J.-P. and Lansson, L., *Ocean Acidification*, Oxford University Press., Oxford, 99–121, 2011.
- Riebesell, U. and Gattuso, J.-P.: Lessons learned from ocean acidification research, *Nat. Clim. Change*, 5, 12–14, 2015.
- Riebesell, U., Lee, K., and Nejstgaard, J. C.: Pelagic mesocosms, in: Riebesell U., Fabry, V. J., Hansson, L., Gattuso, J. P., Guide to best practices for ocean acidification research and data reporting, Office for Official Publications of the European Union, Luxembourg, 95–112, 2010.
- Robbins, L. L., Hansen, M. E., Kleypas, J. A., and Meylan, S. C.: CO₂calc: A User Friendly Carbon Calculator for Windows, Mac OS X and iOS (iPhone), *Open File Rep.*, 2010–1280, 2010.
- Sañudo-Wilhelmy, S. A., Tovar-Sanchez, A., Fu, F. X., Capone, D. G., Carpenter, E. J., and Hutchins, D. A.: The impact of surface-adsorbed phosphorus on phytoplankton Redfield stoichiometry, *Nature*, 432, 897–901, 2004.
- Schulz, K. G., Barcelos e Ramos, J., Zeebe, R. E., and Riebesell, U.: CO₂ perturbation experiments: similarities and differences between dissolved inorganic carbon and total alkalinity manipulations, *Biogeosciences*, 6, 2145–2153, <https://doi.org/10.5194/bg-6-2145-2009>, 2009.
- Semeniuk, D. M., Bundy, R. M., Posacka, A. M., Robert, M., Barbeau, K. A., and Maldonado, M. T.: Using ⁶⁷Cu to study the biogeochemical cycling of copper in the northeast subarctic Pacific ocean, *Front. Mar. Sci.*, 3, 2–19, 2016.
- Shaked, Y. and Lis, H.: Disassembling iron availability to phytoplankton, *Front. Microbiol.*, 3, 123, <https://doi.org/10.3389/fmicb.2012.00123>, 2012.
- Segovia, M., Lorenzo, M. R., Maldonado, M. T., Larsen, A., Berger, S. A., Tsagaraki, T. M., Lázaro, F. J., Iniguez, C., García-Gómez, C., Palma, A., Mausz, M. A., Gordillo, F. J. L., Fernández, J. A., Ray, J. L., and Egge, J. K.: Iron availability modulates the effects of future CO₂ levels within the marine planktonic food web, *Mar. Ecol. Prog. Ser.*, 565, 17–33, 2017.
- Segovia, M., Rosario Lorenzo, M., Iniguez, C., and García-Goimez, C.: Physiological stress response associated with elevated CO₂ and dissolved iron in a phytoplankton community dominated by the coccolithophore *Emiliania huxleyi*, *Mar. Ecol. Prog. Ser.*, 586, 73–89, 2018.

- Shi, D., Xu, Y., Hopkinson, B. M., and Morel, F. M. M.: Effect of ocean acidification on iron availability to marine phytoplankton, *Science*, 327, 676–679, 2010.
- Stocker, T. F., Qin, D., Plattner, G.-K., Tignor, M., Allen, S. K., Boschung, J., Nauels, A., Xia, Y., Bex, V., and Midgley, P. M.: IPCC, 2013: Climate Change 2013: The Physical Science Basis. Contribution of Working Group I to the Fifth Assessment Report of the Intergovernmental Panel on Climate Change, Cambridge University Press, Cambridge, United Kingdom and New York, NY, USA, 1535 pp., 2013.
- Sunda, W. G.: Feedback interactions between trace metal nutrients and phytoplankton in the ocean, *Front. Microbiol.*, 3, 204, <https://doi.org/10.3389/fmicb.2012.00204>, 2012.
- Sunda, W. G. and Huntsman, S. A.: Iron uptake and growth limitation in oceanic and coastal phytoplankton, *Mar. Chem.*, 50, 189–206, 1995a.
- Sunda, W. G. and Huntsman, S. A.: Cobalt and zinc interreplacement in marine phytoplankton: biological and geochemical implications, *Limnol. Oceanogr.*, 40, 1404–1417, 1995b.
- Sunda, W. G. and Huntsman, S. A.: Control of Cd concentrations in a coastal diatom by interactions among free ionic Cd, Zn, and Mn in seawater, *Environ. Sci. Technol.*, 32, 2961–2968, 1998.
- Sunda, W. G. and Huntsman, S. A.: Effect of Zn, Mn, and Fe on Cd accumulation in phytoplankton: implications for oceanic Cd cycling, *Limnol. Oceanogr.*, 45, 1501–1516, 2000.
- Tang, D. G. and Morel, F. M. M.: Distinguishing between cellular and Fe-oxide-associated trace elements in phytoplankton, *Mar. Chem.*, 98, 18–30, 2006.
- Taylor, S.: Abundance of chemical elements in the continental crust: a new table, *Geochim. Cosmochim. Ac.*, 28, 1273–1285, 1964.
- Tovar-Sanchez, A., Sanudo-Wilhelmy, S. A., Garcia-Vargas, M., Weaver, R. S., Popels, L. C., and Hutchins, D. A.: A trace metal clean reagent to remove surface-bound iron from marine phytoplankton, *Mar. Chem.*, 82, 91–99, 2003.
- Twining, B. S. and Baines, S. B.: The trace metal composition of marine phytoplankton, *Ann. Rev. Mar. Sci.*, 5, 191–215, 2013.
- Wells, M. L.: Manipulating iron availability in nearshore waters, *Limnol. Oceanogr.*, 44, 1002–1008, 1999.
- Zamzow, H., Coale, K. H., Johnson, K. S., and Sakamoto, C. M.: Determination of copper complexation in seawater using flow injection analysis with chemiluminescence detection, *Anal. Chim. Acta.*, 377, 133–144, 1998.
- Zondervan, I.: The effects of light, macronutrients, trace metals and CO₂ on the production of calcium carbonate and organic carbon in coccolithophores – A review, *Deep-Sea Res. Pt. II*, 54, 521–537, 2007.